JACS
JOURNAL OF THE AMERICAN CHEMICAL SOCIETY
Article
pubs.acs.org/JACS

Mechanisms of Furfural Reduction on Metal Electrodes: Distinguishing Pathways for Selective Hydrogenation of Bioderived Oxygenates

Xiaotong H. Chadderdon,[†,‡,#] David J. Chadderdon,[†,‡,#] John E. Matthiesen,[†,‡,§] Yang Qiu,[†,‡] Jack M. Carraher,[†,§] Jean-Philippe Tessonnier,[†,‡,§] and Wenzhen Li*[,†,‡]

[†]Department of Chemical and Biological Engineering, Iowa State University, 618 Bissell Road, Ames, Iowa 50011, United States
[‡]US Department of Energy Ames Laboratory, 2408 Pammel Drive, Ames, Iowa 50011, United States
[§]NSF Engineering Research Center for Biorenewable Chemicals (CBiRC), 617 Bissell Road, Ames, Iowa 50011, United States

Supporting Information

ABSTRACT: Electrochemical reduction of biomass-derived platform molecules is an emerging route for the sustainable production of fuels and chemicals. However, understanding gaps between reaction conditions, underlying mechanisms, and product selectivity have limited the rational design of active, stable, and selective catalyst systems. In this work, the mechanisms of electrochemical reduction of furfural, an important biobased platform molecule and model for aldehyde reduction, are explored through a combination of voltammetry, preparative electrolysis, thiol-electrode modifications, and kinetic isotope studies. It is demonstrated that two distinct mechanisms are operable on metallic Cu electrodes in acidic electrolytes: (i) electrocatalytic hydrogenation (ECH) and (ii) direct electroreduction. The contributions of each mechanism to the observed product distribution are clarified by evaluating the requirement for direct chemical interactions with the electrode surface and the role of adsorbed hydrogen. Further analysis reveals that hydrogenation and hydrogenolysis products are generated by parallel ECH pathways. Understanding the underlying mechanisms enables the manipulation of furfural reduction by rationally tuning the electrode potential, electrolyte pH, and furfural concentration to promote selective formation of important biobased polymer precursors and fuels.

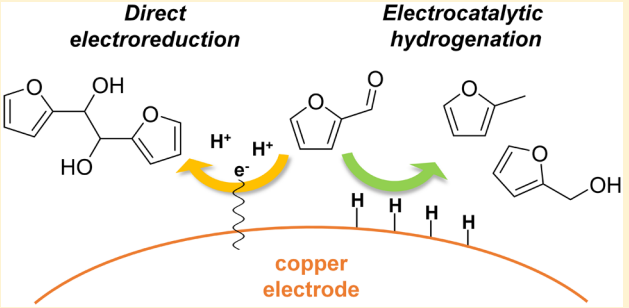

INTRODUCTION

Electrocatalytic hydrogenation (ECH) is emerging as an environmentally friendly approach for the selective reduction of multifunctional chemicals. ECH is analogous to conventional thermocatalytic hydrogenation, with the key difference that adsorbed hydrogen (H_{ads}) is electrochemically generated in situ on the electrode surface by proton or water reduction (Volmer reaction) rather than through the dissociation of molecular H_2.[1] In this way, the kinetic barriers for H_2 activation are avoided and hydrogenations can be performed without the need for external H_2 supply and at mild conditions.[2−4] ECH of carbonyl groups, which are prevalent in important biobased platform chemicals, may yield alcohols by hydrogenation with two H_{ads}, or alkyls through hydrogenation and hydrogenolysis reactions with four H_{ads} (Scheme 1). However, ECH is often in competition with the hydrogen evolution reaction (HER), which consumes H_{ads} through Tafel or Heyrovsky reactions and lowers the faradaic efficiency to ECH.[5]

A significant challenge of performing selective electrocatalytic reductions is the coexistence of direct electroreduction routes (Scheme 1), in which carbonyls participate in electron transfer at the electrode and protonations occur in solution.[6] The

Scheme 1. Proposed Pathways of Electrochemical Reduction of Carbonyls in Acidic Electrolytes

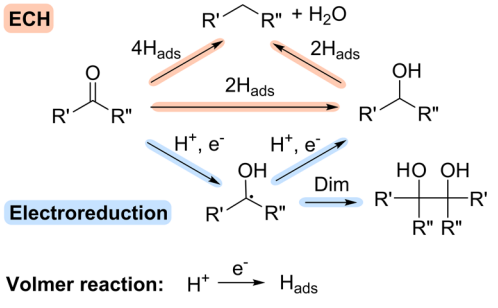

reaction with one H^+/e^- pair generates a radical intermediate ($C^{\bullet}-OH$), which may either dimerize through C−C coupling with a second radical, or be further converted by another H^+/e^- to yield the alcohol product.[6] Alternatively, equal amounts of aldehydes and alcohols may be formed by the disproportiona-

Received: June 18, 2017
Published: September 13, 2017

DOI: 10.1021/jacs.7b06331
J. Am. Chem. Soc. 2017, 139, 14120−14128

tion of C•−OH. The preference for ECH or electroreduction routes is largely determined by the relative potentials required for H_{ads} and C•−OH formation. As a result, ECH is strongly preferred on low hydrogen overpotential electrodes (e.g., platinum-group metals), whereas electroreduction is preferred on high hydrogen overpotential electrodes such as Pb, Hg, Cd, and graphite.[1] However, the two routes may be in competition on electrodes with intermediate hydrogen overpotentials (e.g., Ni, Co, Fe, Cu, Ag and Au), which is a complicating factor for mechanistic studies. In particular, it is not straightforward to determine the pathway of alcohol formation, which may occur through either ECH or electroreduction routes.

Biomass-derived oxygenates have the potential to replace fossil resources as feedstocks for the sustainable production of fuels and chemicals.[7,8] Currently, there is significant interest in the electrochemical conversion of furanic compounds such as furfural and 5-hydroxymethylfurfural (HMF), owing to their versatility as platform chemicals for production of polymers, fine chemicals, and biofuels, and their availability from biomass by the acid-catalyzed dehydration of pentose and hexose sugars, respectively.[9,10] In particular, the selective hydrogenation of the aldehyde groups in furfural or HMF generates furfuryl alcohol (FA) or 2,5-bis(hydroxymethyl)furan (BHMF), respectively (Scheme 2), which are precursors for production of polymers,

Scheme 2. Key Hydrogenation and Hydrogenolysis Products of Furfural and HMF

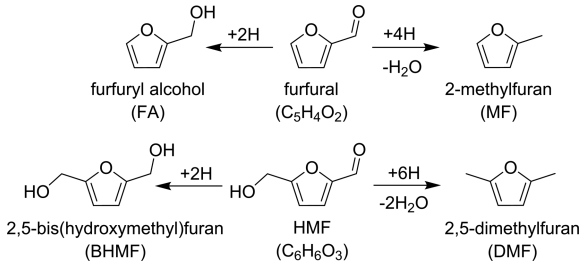

resins, and chemicals.[11] Selective hydrogenolysis generates 2-methylfuran (MF) or 2,5-dimethylfuran (DMF), which are potential liquid transportation fuels.[12,13] It has been demonstrated that the selectivity to hydrogenation or hydrogenolysis products is influenced by the nature of the catalysts, applied potential or current density, electrolyte pH, and initial reactant concentration.[14−20] However, much of the recent literature has focused on proof-of-concepts, and there remain understanding gaps between reaction conditions, underlying mechanisms, and observed product selectivity. Notably, it remains unclear whether hydrogenations occur by H_{ads} at the electrode surface (ECH) or by H^+ in solution (electroreduction).[9,18]

Herein, we investigate the mechanisms for electrochemical reduction of the aldehyde functionality of furfural in acidic electrolytes in order to elucidate the interplay between ECH and electroreduction routes, and their effects on observed product selectivies. Cu was selected as the electrode material because of its unique ability to generate hydrogenolysis products with high selectivity.[14] We demonstrate that both the ECH and electroreduction mechanisms are operable on Cu, leading to formation of FA, MF, and the dimer product hydrofuroin. Electrochemical measurements on electrodes modified with organothiol self-assembled monolayers (SAMs) provide strong evidence that hydrogenation and hydrogenolysis reactions require direct chemical interaction with the electrode surface, whereas hydrofuroin formation is relatively insensitive to the nature of surface. Moreover, observed H/D isotope effects, behavior under proton mass-transport-limited conditions, and a comparative study with a high hydrogen overpotential Pb electrode indicate that H_{ads} is required for hydrogenation and hydrogenolysis reactions, namely by the ECH mechanisms. A pathway study reveals that further reduction of FA to MF is not a significant contribution to the MF observed during the electrolysis of furfural, and instead those products are likely formed by parallel reactions. Finally, the reactions are manipulated by applying knowledge of the underlying mechanisms and tuning reaction conditions to promote selective formation of important chemicals for biobased polymers and fuels synthesis. The techniques used in this work to distinguish different mechanisms are not uniquely applicable to furfural reduction, and can potentially be extended to study other important electrochemical reductions.

METHODS

General Considerations. Furfural (99%), furfuryl alcohol (98%), 2-methylfuran (99%), 3-mercaptopropionic acid (99%), 2-mercaptobenzothiazole (99%), 12-mercaptododecanoic acid (96%), sulfuric acid-d_3 (95−98%, 99.5 atom % D), deuterium oxide (D_2O, 99.9 atom % D), and sodium sulfate (99%), were purchased from Sigma-Aldrich. Acetonitrile (CH_3CN, 99.9% "HPLC grade"), 2-propanol (99.9%), hydrochloric acid (37%), sulfuric acid (98%), and pH buffer solutions (pH 4.00 and 7.00) were purchased from Fisher Scientific. Acetonitrile-d_3 (99.8 atom % D) was obtained from Cambridge Isotope Laboratories, Inc. Water was deionized (18.2 MΩ cm) with a Barnstead E-Pure purification system and used to prepare all electrolytes. Typical electrolytes were 0.5 M sulfuric acid (approximately pH 0.5) or 0.5 M sulfate solutions (pH 1.4−3.0) with 25% v/v CH_3CN cosolvent. Deuterated electrolytes were adjusted to the desired pD according to the widely accepted formula:[21] pD = pH* + 0.40, in which pH* is the reading measured in deuterated electrolyte with a pH meter calibrated in conventional pH buffer solutions.

Electrochemical Measurements. Electrochemical measurements were performed with a Bio-Logic SP-300 electrochemical workstation. A double-junction Ag/AgCl (Pine Research Instrumentation) and a graphite rod (Pine Research Instrumentation) were used as the reference and counter electrodes, respectively. The reference electrode was calibrated against a reversible hydrogen electrode (RHE, eDAQ) and all potentials herein are reported on the RHE reference scale. Electrolyte pH was measured with a hand-held pH meter (Hanna HI98103) calibrated in conventional pH buffer solutions. Solution resistance between working and reference electrodes was measured by potentiostatic electrochemical impedance spectroscopy and compensated (85%) by the electrochemical workstation.

Cyclic voltammetry was performed on a Cu rotating disk electrode (RDE, 5.0 mm diameter, Pine Research Instrumentation) at 2500 rpm. The RDE was polished with an alumina suspension (0.3 μm, Allied High Tech Products, Inc.) on a microcloth polishing disk (Buehler) and cleaned with DI water in an ultrasonic bath before each use. The electrolyte was purged with nitrogen gas before and during measurements. Cyclic voltammograms were collected using a 50 mV s^{-1} sweep rate.

Preparative electrolysis was performed in an H-cell reactor with anode and cathode chambers separated by a Nafion 212 proton exchange membrane (PEM). Cathode electrolyte was purged with argon gas (99.999%, Airgas, Inc.) throughout the reaction to remove dissolved gases and evolved H_2, and to strip the volatile product MF into a two-chamber cold trap filled with CH_3CN and cooled to −10 °C. Cu foils (0.127 mm thick, 99.9%, Alfa Aesar) were used as electrodes for preparative electrolysis immediately after pretreatment by a cleaning sequence of 2-propanol, deionized water, dilute hydrochloric acid, and deionized water. Pb foils (0.76 mm thick, 99.8%, Alfa Aesar) were mechanically polished with 600 grit sandpaper and cleaned with laboratory tissue. Unless noted otherwise, the

DOI: 10.1021/jacs.7b06331
J. Am. Chem. Soc. 2017, 139, 14120−14128

exposed geometric surface area of electrodes was maintained at 5.0 cm^2, accounting for both the front and back sides. Preparative electrolysis was performed in 20 mL of electrolyte which was stirred at 1000 rpm with a magnetic stir bar. For studying the effect of furfural initial concentration, a short reaction time of 30 min was used to make comparisons at low degrees of conversion and relatively constant bulk furfural concentrations. All reactions were performed at room temperature (23 ± 1 °C).

Product Analysis. After preparative electrolysis reactions, liquid aliquots were collected from the reactor chamber and cold trap and diluted in water or CH_3CN for analysis by high-performance liquid chromatography (HPLC). Hydrogen gas was quantified with a gas chromatograph connected to the outlet of the cold trap. Hydrofuroin (1,2-di(furan-2-yl)ethane-1,2-diol) was identified by ^1H NMR and mass spectrometry (MS), and quantified by HPLC. Two isomers of hydrofuroin are reported together for simplicity. Product analysis details and calculations of selectivity and faradaic efficiency are included in Supporting Information.

RESULTS AND DISCUSSION

Distinguishing ECH and Electroreduction Mechanisms. The first challenge in bridging the understanding gaps between mechanisms, reaction conditions, and selectivity for the electrochemical reduction of carbonyl groups is to clarify which mechanisms are responsible for hydrogenation, hydrogenolysis, and hydrodimerization products. Electrodes modified with SAMs of organothiols were employed to experimentally determine the nature of electrode processes responsible for formation of each product. ECH involves strong interactions of reacting species with the electrode surface and requires H_{ads} as the hydrogen source. The electron transfer (ET) for H_{ads} formation is defined as an inner-sphere electrode process, and as such is highly dependent on the electrode surface properties.[5] However, for the electroreduction mechanism, protonations occur in solution, and the heterogeneous ET may proceed by either inner-sphere or outer-sphere processes. Outer-sphere reactions do not require strong interactions between reactants and the electrode surface and ET occurs by electron tunneling.[22,23] Therefore, outer-sphere reactions are generally less dependent on the nature of the electrode material. Organic SAMs inhibit inner-sphere ET and ECH reactions by preventing free diffusion of electroactive species and their direct access to the electrode surface, but have only a small effect on outer-sphere ET rates if the layers are sufficiently thin for facile electron tunneling.[24−26] For the electroreduction pathway, the reduction of furfural is expected to be unaffected by such SAM-modifications if it occurs by an outer-sphere ET process.

Three organothiols that readily form compact SAMs on Cu[27−31] were selected to modify the electrodes: two carboxyl-terminated alkanethiols with different chain lengths (C3 and C12), namely 3-mercaptopropionic acid (MPA) and 12-mercaptododecanoic acid (MDA) and a heterocyclic 2-mercaptobenzothiazole (MBT). Electron tunneling resistance has an exponential dependence on tunneling distance, which is determined by the molecular length of the SAMs.[32] As a result, outer-sphere ET processes are suppressed on surfaces blocked by long-chain linear alkanethiols (e.g., MDA, C12) SAMs, whereas they are essentially unaffected on surfaces blocked by short-chains (e.g., MPA, C3).[24] Furthermore, SAMs of conjugated molecules like MBT may be particularly effective at blocking surface sites and inner-sphere ET, while still allowing electron tunneling (outer-sphere ET).[33−36]

HER can serve as a probe reaction to evaluate the quality of the SAMs and their effectiveness to inhibit ET.[37,38] Cyclic voltammetry revealed a significant decrease in HER and double-layer charging (capacitive) currents on thiol-modified Cu electrodes (Figure 1a), indicating that the SAMs inhibited

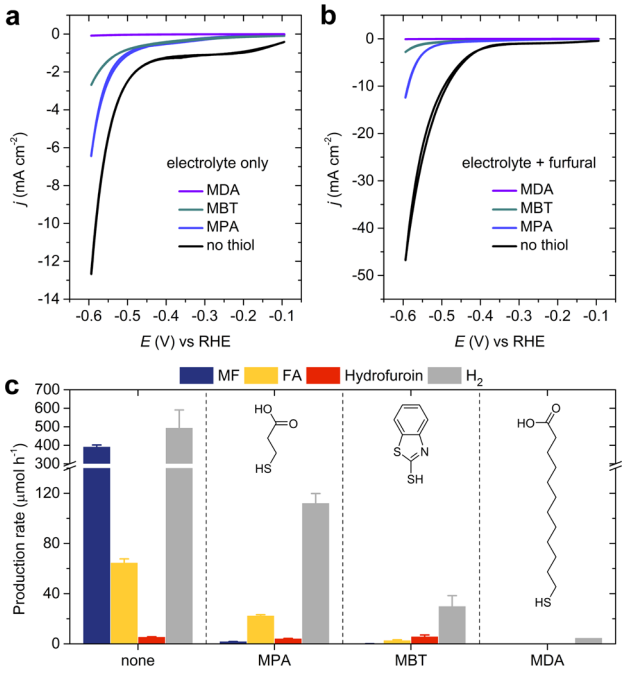

Figure 1. (a) Cyclic voltammograms on a Cu RDE in pH 0.5 electrolyte with or without the addition of 0.25 mM MPA, MBT, or MDA and (b) with addition of 0.05 M furfural. (c) Observed production rates during preparative electrolysis of furfural on Cu, Cu-MPA, Cu-MBT, and Cu-MDA electrodes. Conditions: 0.05 M furfural and 0.25 mM of the indicated organothiol, pH 0.5 electrolyte, 1 h duration, $E = -0.55$ V.

access to electrochemically active Cu surface sites. The degree of current suppression was in the order of MPA < MBT ≪ MDA, with MDA nearly completely blocking both faradaic and nonfaradaic processes. Longer-chain thiols, such as MDA, assemble into complete and impenetrable SAMs owing to their stronger van der Waals intermolecular attractions,[39] and as noted their SAMs are of sufficient thickness to inhibit electron tunneling. SAMs of MPA and MBT would be expected to completely suppress inner-sphere reactions, so the fact that HER current was observed suggests that those films are incomplete or contain pinhole defects which allow access to some active metal sites. MBT was more effective at inhibiting HER than MPA, likely owing to the stronger intermolecular attractions of its aromatic structure.[40] The same trend of current suppression was observed in the presence of furfural (Figure 1b), demonstrating that the thiol-modified electrodes also reduced the overall rate of furfural reduction.

Constant-potential preparative electrolysis of furfural conducted in pH 0.5 electrolyte confirmed that both furfural reduction and HER were inhibited by the SAMs. Moreover, the distribution of furfural reduction products was very sensitive to surface modifications, as shown in Figure 1c. FA and MF production rates were severely suppressed on thiol-modified electrodes; for example, FA decreased from 64.5 to 2.7 μmol h^{-1} and MF decreased from 391.0 to <0.1 μmol h^{-1} on Cu-MBT compared to unmodified Cu. Similar results were

DOI: 10.1021/jacs.7b06331
J. Am. Chem. Soc. 2017, 139, 14120−14128

obtained in a pH 3.0 electrolyte, in which FA and MF were both suppressed on SAM-modified electrodes (Figure S2). Only trace amounts of furfural reduction products or H_2 were detected on the MDA-Cu electrode, confirming that C12 thiol SAMs block nearly all the electrode reactions. These results indicate that hydrogenation and hydrogenolysis pathways to FA and MF require direct interaction of reactants with the Cu surface. In contrast, hydrofuroin formation rate was remarkably unchanged on MPA-Cu (decreased 24%) and MBT-Cu (increased 6.1%) compared to the unmodified Cu, strongly suggesting that the first e^- transfer of the electroreduction pathway may occur through outer-sphere ET, which does not require specific adsorption of furfural or H.

Electrochemical experiments performed with H/D isotopically substituted solvents and electrolytes were performed to further elucidate the mechanisms of furfural hydrogenation and hydrogenolysis. Kinetic isotopic effects (KIE) have been observed for HER on many electrode materials, including Cu, where the kinetics (i.e., exchange current density) of HER are greater than deuterium evolution reaction (DER).[41] This is exemplified by the cathodic shift between the HER/DER waves (e.g., 87 mV at 10 mA cm^{-2}) in deuterated electrolytes, shown in Figure 2a. A normal KIE is also expected for the ECH

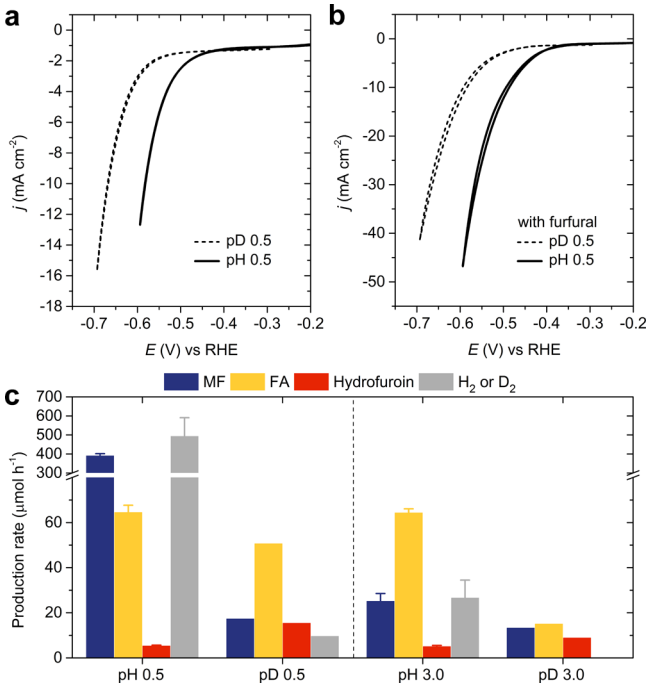

Figure 2. (a) Cyclic voltammograms on a Cu RDE in pH 0.5 or pD 0.5 electrolytes and (b) with addition of 0.05 M furfural. (c) Observed production rates during preparative electrolysis of furfural on Cu electrodes in H- or D-electrolytes. Conditions: 0.05 M furfural, 1 h duration, $E = -0.55$ V.

mechanism, which shares a common step with HER (Volmer reaction) and also involves reactions with H_{ads}. The voltammograms in Figure 2b show that furfural reduction experiences a KIE, and that its magnitude is similar to the KIE for HER (e.g., 98 mV shift at 10 mA cm^{-2}). Production rates for MF and FA determined by preparative electrolysis at −0.55 V decreased by 95.6% and 21.5% in pD 0.5 electrolyte, respectively, compared to pH 0.5 (Figure 2c). We rationalize that the relatively minor decrease in FA rate compared to MF is attributed to a selectivity change from MF to FA under deuterated conditions. Analogous experiments performed at pH 3.0, a condition at which FA is the major product, showed that the production rates for both MF and FA were significantly decreased (47.1% and 76.6%, respectively) in D-electrolyte compared to H-electrolyte. In contrast, the rate of hydrofuroin production actually increased in D-electrolyte compared to H-electrolyte at both pH (or pD) conditions, which may be a result of an equilibrium-shift for a preceding homogeneous reaction (e.g., protonation) due to thermodynamic isotope effects.[42] These results are consistent with the behavior expected if MF and FA are from ECH reactions and hydrofuroin is from electroreduction, and therefore are in agreement with the study on thiol-modified electrodes.

ECH and electroreduction mechanisms can be further distinguished by studying furfural reduction under a special case of mass-transport-limited conditions. The rates of reactions which consume protons at the electrode/electrolyte interface (e.g., HER and ECH) can become completely mass-transport-limited in mildly acidic conditions at moderate current densities, owing to the low bulk proton concentrations. This is shown by the rotating-disk voltammogram in Figure 3a,

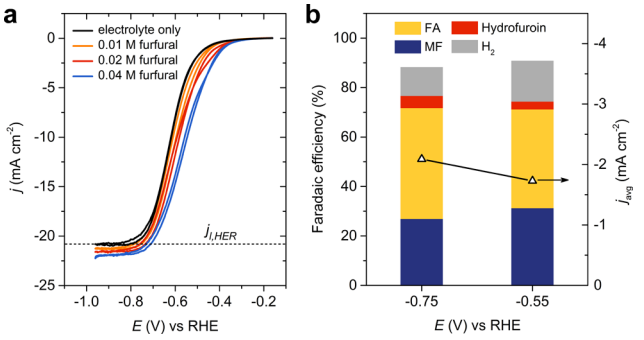

Figure 3. (a) Cyclic voltammograms on a Cu RDE in pH 3.0 electrolyte with various furfural concentrations. Baseline correction was performed to remove the contribution of double-layer charging currents. (b) Faradaic efficiency to furfural reduction products and H_2 measured from preparative electrolysis. Conditions: pH 3.0 electrolyte, 0.05 M furfural, 1 h duration.

in which the rate of HER plateaus to a mass-transport-limited current density ($j_{l,HER}$) of −20.9 mA cm^{-2} in a pH 3.0 electrolyte. Similarly, ECH reactions consume interfacial protons through the Volmer reaction ($H^+ + e^- \rightarrow H_{ads}$). Consequently, if furfural reduction proceeds solely by ECH, it would also be subject to proton transport limitations and its rate would be limited accordingly. In contrast, if furfural reduction proceeds only by electroreduction, in which protonations occur in the bulk solution, its rate would not be limited by proton transport to the electrode surface. This has been demonstrated for the similar case of benzaldehyde electroreduction, for which the mass-transport-limited current was proportional to substrate concentration, even in very mildly acidic conditions (i.e., pH 5.2).[43] Preparative electrolysis results (Figure 3b) show that H_2, FA, MF, and hydrofuroin formation accounted for 11.6%, 44.8%, 26.9%, and 4.9% of the total current at −0.75 V, a potential within the transport-limited region under electrolysis conditions (Figure S4). Assuming that FA and MF are from ECH reactions and hydrofuroin is from electroreduction, this would indicate that the vast majority of the total current should be subject to proton transport

DOI: 10.1021/jacs.7b06331
J. Am. Chem. Soc. 2017, 139, 14120−14128

limitations (i.e., 83.3% to H_2, FA, and MF), while a minor fraction would not (i.e., 4.9% to hydrofuroin). Figure 3a shows that mass-transport-limited furfural reduction current was remarkably similar to $j_{l,HER}$, and increased only slightly as furfural concentration was increased (e.g., +5.2% difference with 0.04 M furfural). Therefore, the comparison between mass-transport-limited currents for HER and furfural reduction is very consistent with the proposal that FA and MF are products of ECH and hydrofuroin is from electroreduction. Moreover, Figure 3b shows that the product distribution was nearly identical at lower potentials (e.g., −0.55 V), which is evidence that these mechanisms are applicable within the potential range of interest.

Additional mechanistic insight may be gained by comparing Cu to a different electrode material on which direct electroreduction mechanisms are known to dominate. Pb electrodes are commonly used to perform electroreductions without competition from interfering reactions (e.g., HER or electrocatalytic reactions), owing to their weak hydrogen adsorption properties.[44] In fact, the onset potential for furfural reduction on Pb is over 400 mV more positive than for HER (Figure S5), indicating that H_{ads} does not participate in furfural reduction. Hydrofuroin was the major detected product from preparative electrolysis at −0.55 V on Pb, corresponding to faradaic efficiencies of 34% and 38% at pH 0.5 and pH 3.0, respectively (Figure 4). On the other hand, no H_2 or MF, and

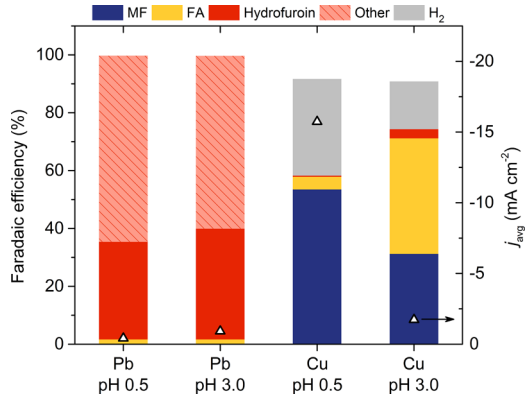

Figure 4. Comparison of the preparative electrolysis of furfural on Pb or Cu electrodes. Conditions: 0.05 M furfural, 1 h duration, E = −0.55 V.

very little FA (<2% faradaic efficiency), was detected under these conditions. A resinous precipitate in the reactor and unidentified peaks in the product chromatographs were observed which were not identified or quantified in this work, but likely contributed to the low total faradaic efficiencies to detected products. Such products have been previously observed during electrochemical furfural reduction,[16,45] and may be other dimer or oligomer byproducts of electroreduction reactions.[46] Figure 4 also shows that the products observed on Pb were distinctly different than on Cu, in which FA and MF were the main products. This is further evidence that FA and MF formation requires H_{ads} and occurs through ECH mechanisms on Cu.

Reaction Pathways. It has been previously implied that MF is a secondary product of furfural reduction on Cu, with FA formed as an intermediate under electrochemical conditions.[14,16,19] This would suggest that ECH product selectivity can be tuned by varying the extent of reaction, with MF preferred at high conversion after subsequent hydrogenolysis of FA. In clear contradiction, we found that FA and MF selectivities were remarkably constant with respect to reaction duration and degree of furfural conversion (Figure 5a), which suggests that the two products are mainly generated from parallel, not consecutive reactions, on Cu electrodes.

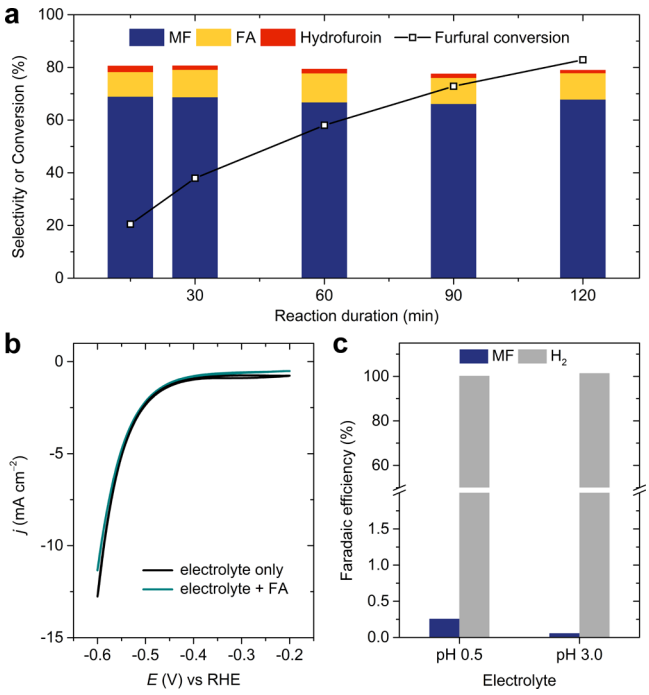

Figure 5. (a) Conversion and selectivity over time during the preparative electrolysis of furfural on Cu. Conditions: 0.05 M furfural, pH 0.5 electrolyte, E = −0.55 V. Each bar represents an independent experiment. (b) Cyclic voltammograms on a Cu RDE in pH 0.5 electrolyte with or without addition of 0.01 M FA. (c) Faradaic efficiency to MF and H_2 during the preparative electrolysis of 0.01 M FA performed on Cu. Conditions: pH 0.5 or 3.0 electrolytes, 1 h duration, E = −0.55 V.

The cyclic voltammogram of FA was nearly identical to that of the blank electrolyte, which suggests that HER was the dominant electrode reaction in the presence of FA (Figure 5b). Preparative electrolysis of FA resulted in ca. 100% efficiency to HER at −0.55 V at both pH 0.5 and 3.0, whereas only a negligible amount of MF was detected corresponding to <1% efficiency (Figure 5c). An initial FA concentration of 0.01 M was chosen to represent typical bulk concentrations present during furfural reduction. These results indicate that hydrogenolysis of FA is very slow under these conditions; therefore, the large amount of MF produced during furfural reduction is formed in parallel with FA, rather than from the decoupled sequential reduction of FA product.

Insight into feasible pathways for MF formation which bypass the FA intermediate was obtained by Shi et al., who explored the catalytic conversion of furfural to FA and MF on Cu(111) surfaces on the basis of density functional theory (DFT) calculations.[47] They found that H addition or decomposition pathways of the preferred monohydrogenated alkoxyl intermediate (C_4H_3O−CH_2O) had similar energy barriers (1.17 and 1.18 eV, respectively) and thermodynamic free energy changes (0.24 and 0.33 eV, respectively), and therefore parallel routes to FA or MF through this intermediate

DOI: 10.1021/jacs.7b06331
J. Am. Chem. Soc. 2017, 139, 14120−14128

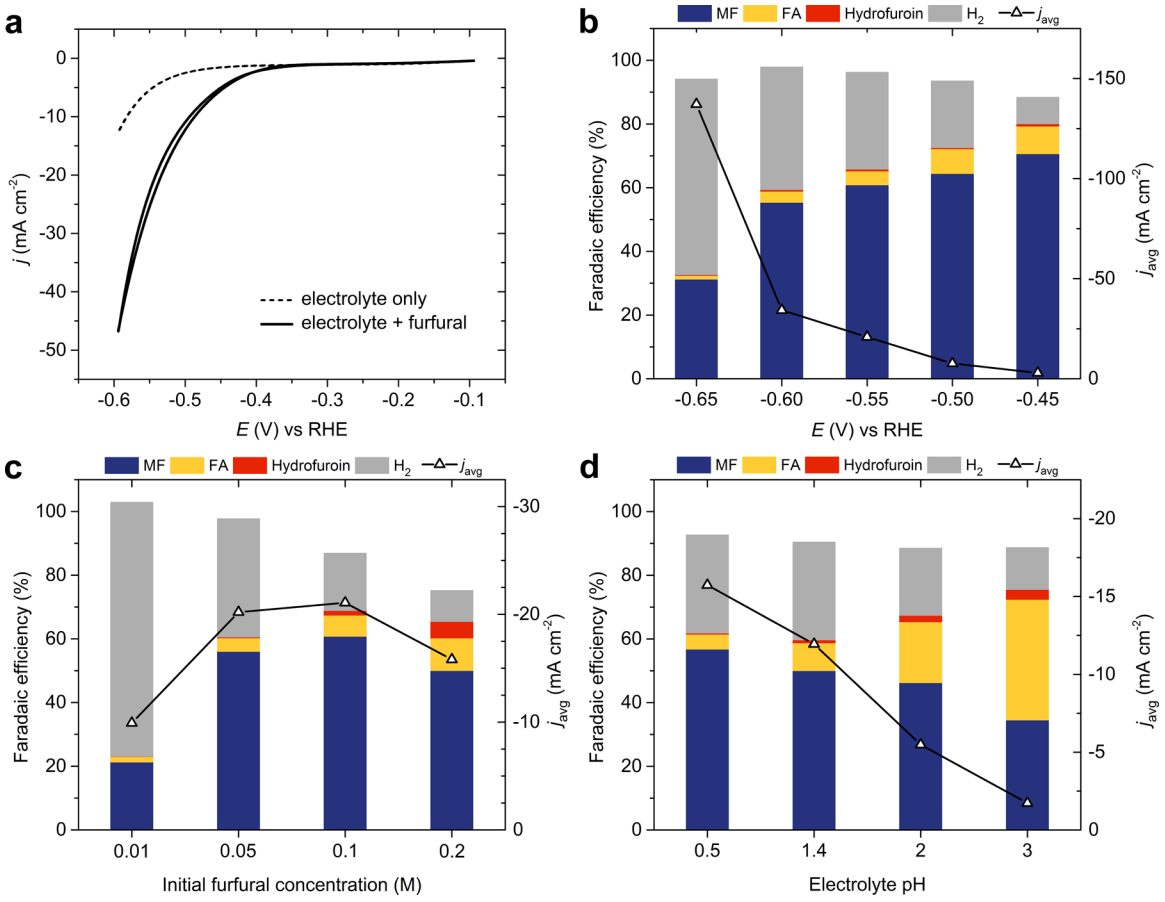

Figure 6. (a) Cyclic voltammograms on a Cu RDE in pH 0.5 electrolyte with or without the addition of 0.05 M furfural. (b) Preparative electrolysis of furfural at varying cathode potentials. Conditions: 0.05 M furfural, pH 0.5 electrolyte, 144 C charge transferred, electrode area was 2.5 cm^2 for −0.6 and −0.65 V. (c) Preparative electrolysis of furfural with various initial furfural concentrations. Conditions: pH 0.5 electrolyte, 30 min duration, E = −0.55 V. (d) Preparative electrolysis of furfural with electrolytes ranging from pH 0.5 to 3.0. Conditions: 0.05 M furfural, 1 h duration, E = −0.55 V.

should be competitive. Comprehensive DFT modeling of furfural conversion under electrochemical conditions and in situ spectroscopy should be focuses of future work to confirm the pathway.

Impact of Reaction Conditions. The efficiency and selectivity of furfural reduction can be manipulated by applying knowledge of the underlying mechanisms to rationally choose experimental conditions such as electrode potential, reactant concentration, and electrolyte pH. The faradaic efficiency for furfural reduction is determined by its kinetic competition with HER. It is generally accepted that HER on Cu occurs by the Volmer−Heyrovsky mechanism,[5] shown in eqs 1−2 for acidic electrolytes.

$$H^+ + e^- \rightarrow H_{ads} \quad (1)$$

$$H_{ads} + H^+ + e^- \rightarrow H_2 \quad (2)$$

The present work provides strong evidence that FA and MF are produced by ECH reactions through parallel hydrogenation and hydrogenolysis pathways. Accordingly, their formation rates will be dependent on the surface coverages of both H_{ads} and furfural adsorbates.[3] The surface coverage of H_{ads} is determined by the relative kinetics of its adsorption and desorption (eqs 1−2), which are potential-dependent electrochemical reactions, as well as the nonelectrochemical reaction between furfural adsorbates and H_{ads}. Therefore, the rate of ECH will depend on potential and other factors which influence H_{ads} and furfural adsorbate coverage, including furfural concentration and electrolyte pH. Hydrofuroin formation via the electroreduction mechanism does not involve H_{ads}; however its formation is also dependent on potential, substrate concentration, and electrolyte pH.[48] Furthermore, it was shown in this work that the ET preceding dimerization can occur by an outer-sphere process, and is not sensitive to the presence of surface adsorbates.

The onset potential of furfural reduction on Cu is about −0.35 V, as shown by the increased cathodic current in the presence of furfural compared to HER (Figure 6a). Preparative electrolysis was performed at constant potentials ranging from −0.45 to −0.65 V. Figure 6b shows that FA and MF were the main furfural reduction products over the evaluated potential range, indicating that there was sufficient H_{ads} on the electrode surface for the ECH mechanism to dominate under these conditions (i.e., pH 0.5, initial furfural concentration 0.05 M). Accordingly, hydrofuroin formation via the electroreduction mechanism was minor, with typically less than 2% faradaic efficiency. The total current density increased in magnitude at more negative potentials; however, faradaic efficiency to furfural reduction decreased significantly, corresponding to an increase in H_2 production. The rate of the Volmer reaction (eq 1) is enhanced at more negative potentials, resulting in a greater total availability of H_{ads} for HER or ECH. However, HER will

DOI: 10.1021/jacs.7b06331
J. Am. Chem. Soc. 2017, 139, 14120−14128

outpace ECH at more negative potentials because the rate constant of the Heyrovsky reaction (eq 2) increases exponentially with potential, whereas the reaction between furfural adsorbates and H_{ads} is nonelectrochemical, and the rate constant is potential-independent. Cathode potential also influenced the ECH selectivity, with the preference for MF more pronounced at increasingly negative potentials, as seen qualitatively by the relative faradaic efficiencies of MF and FA in Figure 6b. Electrode potential regulates charge transfer kinetics, surface states, and stability of adsorbed species, and therefore can have significant influence on the selectivity of complex multistep reactions.[49]

The influence of initial furfural concentration was evaluated over the range of 0.01 to 0.2 M in pH 0.5 electrolytes. Figure 6c shows that the competition between furfural reduction and HER was highly dependent on furfural concentration, evidenced by the decrease in faradaic efficiency to HER from 80.0% to 9.9% over the evaluated concentration range. Increasing bulk furfural concentration generally facilitated higher surface coverage of furfural adsorbates, and consequently enhanced rates of ECH reactions forming FA and MF. Conversely, the rate of HER was decreased owing to the increased competition for available H_{ads}. Interestingly, the ECH rate actually decreased when furfural concentration was further increased from 0.1 to 0.2 M, indicating that the electrode surface became oversaturated with furfural-related adsorbates. In contrast, the rate of hydrofuroin formation, which does not require H_{ads}, increased steadily over the range of furfural concentrations. Additionally, the selectivity of ECH reactions was sensitive to furfural concentration, as the molar ratio of MF to FA products decreased from ca. 6.2 at 0.01 M to 2.4 at 0.2 M furfural concentration. Unidentified products were also observed after tests in which greater hydrofuroin formation occurred (e.g., 0.1 and 0.2 M furfural), and likely contributed to the lower total faradaic efficiencies at those conditions, similarly to the previously mentioned results of furfural reduction on Pb electrodes.

Varying electrolyte pH had a significant effect on the selectivity and efficiency of furfural reduction, as shown by the preparative electrolysis results at −0.55 V in Figure 6d. The different pH conditions were compared at a constant potential versus the pH-corrected RHE reference scale in order to account for the change in equilibrium reduction potentials with electrolyte pH. Even so, the rates of HER and ECH decreased notably with increasing electrolyte pH, which can be rationalized by considering mass transport effects. HER and ECH consume protons at the electrode/electrolyte interface and can become mass-transport-limited if proton transport from the bulk solution is insufficient, as is the case in mildly acidic electrolytes (e.g., pH 3.0, see Figure S4). In contrast, the rate of hydrofuroin formation, which does not require surface hydrogen, was not notably affected by pH. The increased faradaic efficiency to hydrofuroin at higher pH can be attributed to the lower relative contributions from ECH and HER. The preference to FA or MF was very sensitive to changes in electrolyte pH, which suggests that the electrocatalytic hydrogenation and hydrogenolysis pathways may have different pH dependences. MF was preferred at low pH, whereas FA was the major product at pH 3.0 (FA/MF molar ratio = 2.6). It has been previously suggested that the ratio of hydrogenation and hydrogenolysis products of ECH reactions is sensitive to the presence of metal ions, such as Na^+, in electrolytes.[50] However, this effect is unlikely to explain the present results because the same selectivity trends were observed when sodium sulfate electrolytes were replaced with dilute sulfuric acid electrolytes (Figure S3). The increased selectivity to FA at higher pH may be a result of the lower relative availability of H_{ads} compared to furfural adsorbates. As previously discussed, the rates of HER and ECH reactions decreased at higher pH owing to limited availability of protons at the electrode/electrolyte interface. It is plausible that the competition between the hydrogenation pathway to FA, which requires two H_{ads}, and the hydrogenolysis pathway to MF, in which four H_{ads} participate, could be sensitive to the relative availability of H_{ads} and furfural adsorbates. This explanation would also be consistent with the initial concentration study (Figure 6c), in which MF was more favorable at lower furfural concentrations, which facilitate higher coverage of H_{ads} relative to furfural adsorbates. However, without direct analysis of surface species the exact nature of this selectivity change remains a focus for future investigations.

CONCLUSIONS

The electrochemical reduction of furfural in acidic electrolytes was explored with the goals of distinguishing mechanisms of product formation and bridging understanding gaps between mechanisms, reaction conditions, and product selectivity. Electrodes modified with organothiol SAMs were utilized to determine the requirement for direct interactions between reactants and the electrode surface, and the nature of heterogeneous ET responsible for formation of hydrogenation, hydrogenolysis, and hydrodimerization products. FA and MF formation were inhibited on electrodes modified with MPA and MBT, which indicates those processes require direct interaction with the electrode surface. In comparison, hydrofuroin formation was unaffected, which suggests that the first electron transferred in the electroreduction mechanism, prior to dimerization, is an outer-sphere process and is therefore insensitive to the electrode surface properties or catalytic activity. Production rates of FA and MF exhibited a notable H/D isotope effect, which strongly suggests they are formed through the ECH mechanism by a reaction with electrochemically adsorbed H (or D). An investigation of furfural reduction under proton mass-transport-limited conditions by RDE voltammetry revealed that MF and FA formation consume protons at the electrode/electrolyte interface, consistent with the ECH mechanism. A comparison of the products formed on a Cu electrode to those formed on a high hydrogen overpotential Pb electrode provided additional evidence that MF and FA formation require H_{ads}, through the ECH mechanism. A pathway study revealed that hydrogenation and hydrogenolysis products, FA and MF, are formed mainly through parallel reactions, in which FA is not a major intermediate for MF formation. Finally, understanding of the underlying mechanisms enabled the manipulation of electrochemical furfural reduction by rationally tuning the electrode potential, electrolyte pH, and furfural concentration to promote selective formation of important chemicals for biobased polymers and fuels production. Collectively, these studies highlight the decisive role that reaction conditions play in determining the selectivity of ECH reactions of bioderived oxygenates to hydrogenation or hydrogenolysis products, and the competition between ECH, electroreduction, and HER pathways.

DOI: 10.1021/jacs.7b06331
J. Am. Chem. Soc. 2017, 139, 14120−14128

■ ASSOCIATED CONTENT

Supporting Information

The Supporting Information is available free of charge on the ACS Publications website at DOI: 10.1021/jacs.7b06331.

Experimental details, ^{1}H NMR and MS characterizations for hydrofuroin, supplemental voltammetry and preparative electrolysis results (PDF)

■ AUTHOR INFORMATION

Corresponding Author

*wzli@iastate.edu

ORCID

Jean-Philippe Tessonnier: 0000-0001-9035-634X

Wenzhen Li: 0000-0002-1020-5187

Author Contributions

#X.H.C. and D.J.C. contributed equally.

Notes

The authors declare no competing financial interest.

■ ACKNOWLEDGMENTS

This research was funded by NSF-CBET 1512126. W.L. acknowledges the Iowa State University Start-Up Fund, Ames Laboratory Start-Up Fund, Iowa Energy Center, Bailey Research Career Development Award, and Richard Seagrave Professorship. We thank Dr. Sarah Cady (ISU Chemical Instrumentation Facility) for training and assistance pertaining to the AVIII-600 results included in this publication. We are thankful for fruitful discussions with Prof. Kurt Hebert, Prof. Brent Shanks, and Dr. Toni Pfennig from Iowa State University, and exchange of ideas with Prof. Bin Liu and Nannan Shan from Kansas State University. X.H.C. and D.J.C. are grateful to undergraduate researchers Hyunjin Moon, Aimee Pierce, Geng Sun, and Yuan Tan from Iowa State University for their assistance.

■ REFERENCES

(1) Lessard, J. Electrocatalytic Hydrogenation. In *Organic Electrochemistry*, 5th ed.; Hammerich, O., Speiser, B., Eds.; CRC Press: Boca Raton, FL, 2015; pp 1658−1664.

(2) Coche, L.; Moutet, J.-C. *J. Am. Chem. Soc.* **1987**, *109*, 6887−6889.

(3) Chapuzet, J. M.; Lasia, A.; Lessard, J. Electrocatalytic Hydrogenation of Organic Compounds. In *Electrocatalysis*; Lipkowski, J., Ross, P. N., Eds.; Wiley-VCH: New York, 1998; pp 155−159.

(4) Suastegui, M.; Matthiesen, J. E.; Carraher, J. M.; Hernandez, N.; Quiroz, N. R.; Okerlund, A.; Cochran, E. W.; Shao, Z.; Tessonnier, J.-P. *Angew. Chem., Int. Ed.* **2016**, *55*, 2368−2373.

(5) Schmickler, W.; Santos, E. Hydrogen reaction and electrocatalysis. In *Interfacial Electrochemistry*, 2nd ed.; Schmickler, W., Santos, E., Eds.; Springer-Verlag: Berlin, 2010; pp 163−164.

(6) Ludvík, J. Reduction of Aldehydes Ketones and Azomethines. In *Organic Electrochemistry*, 5th ed.; Hammerich, O., Speiser, B., Eds.; CRC Press: Boca Raton, FL, 2015; pp 1202−1205.

(7) Jiang, Y.; Wang, X.; Cao, Q.; Dong, L.; Guan, J.; Mu, X. Chemical Conversion of Biomass to Green Chemicals. In *Sustainable Production of Bulk Chemicals*, 1st ed.; Xian, M., Ed.; Springer: Dordrecht, 2016; p 19.

(8) Chheda, J. N.; Huber, G. W.; Dumesic, J. A. *Angew. Chem., Int. Ed.* **2007**, *46*, 7164−7183.

(9) Kwon, Y.; Schouten, K. J. P.; van der Waal, J. C.; de Jong, E.; Koper, M. T. M. *ACS Catal.* **2016**, *6*, 6704−6717.

(10) Binder, J. B.; Raines, R. T. *J. Am. Chem. Soc.* **2009**, *131*, 1979−1985.

(11) Jiang, Y.; Woortman, A. J.; Alberda van Ekenstein, G. O.; Petrović, D. M.; Loos, K. *Biomacromolecules* **2014**, *15*, 2482−2493.

(12) Thananatthanachon, T.; Rauchfuss, T. B. *Angew. Chem., Int. Ed.* **2010**, *49*, 6616−6618.

(13) Bohre, A.; Dutta, S.; Saha, B.; Abu-Omar, M. M. *ACS Sustainable Chem. Eng.* **2015**, *3*, 1263−1277.

(14) Nilges, P.; Schröder, U. *Energy Environ. Sci.* **2013**, *6*, 2925−2931.

(15) Roylance, J. J.; Kim, T. W.; Choi, K.-S. *ACS Catal.* **2016**, *6*, 1840−1847.

(16) Jung, S.; Biddinger, E. J. *ACS Sustainable Chem. Eng.* **2016**, *4*, 6500−6508.

(17) Kwon, Y.; de Jong, E.; Raoufmoghaddam, S.; Koper, M. T. M. *ChemSusChem* **2013**, *6*, 1659−1667.

(18) Kwon, Y.; Birdja, Y. Y.; Raoufmoghaddam, S.; Koper, M. T. M. *ChemSusChem* **2015**, *8*, 1745−1751.

(19) Li, Z.; Kelkar, S.; Lam, C. H.; Luczek, K.; Jackson, J. E.; Miller, D. J.; Saffron, C. M. *Electrochim. Acta* **2012**, *64*, 87−93.

(20) Parpot, P.; Bettencourt, A. P.; Chamoulaud, G.; Kokoh, K. B.; Belgsir, E. M. *Electrochim. Acta* **2004**, *49*, 397−403.

(21) Glasoe, P. K.; Long, F. A. *J. Phys. Chem.* **1960**, *64*, 188−190.

(22) Bard, A. J.; Faulkner, L. R. *Electrochemical Methods: Fundamentals and Applications*, 2nd ed.; John Wiley & Sons, Inc.: New York, 2001; p 116.

(23) Schmickler, W.; Santos, E. Theoretical considerations of electron-transfer reactions. In *Interfacial Electrochemistry*, 2nd ed.; Schmickler, W., Santos, E., Eds.; Springer-Verlag: Berlin, 2010; p 99.

(24) Xiao, X.; Pan, S.; Jang, J. S.; Fan, F.-R. F.; Bard, A. J. *J. Phys. Chem. C* **2009**, *113*, 14978−14982.

(25) Bard, A. J. *J. Am. Chem. Soc.* **2010**, *132*, 7559−7567.

(26) Love, J. C.; Estroff, L. A.; Kriebel, J. K.; Nuzzo, R. G.; Whitesides, G. M. *Chem. Rev.* **2005**, *105*, 1103−1169.

(27) Tan, Y. S.; Srinivasan, M. P.; Pehkonen, S. O.; Chooi, S. Y. M. *J. Vac. Sci. Technol., A* **2004**, *22*, 1917−1925.

(28) Arkhipushkin, I. A.; Pronin, Y. E.; Vesely, S. S.; Kazansky, L. P. *Int. J. Corros. Scale Inhib.* **2014**, *3*, 78−88.

(29) Woods, R.; Hope, G. A.; Watling, K. *J. Appl. Electrochem.* **2000**, *30*, 1209−1222.

(30) Marconato, J. C.; Bulhões, L. O.; Temperini, M. L. *Electrochim. Acta* **1998**, *43*, 771−780.

(31) Täubert, C. E.; Kolb, D. M.; Memmert, U.; Meyer, H. *J. Electrochem. Soc.* **2007**, *154*, D293−D299.

(32) Wang, W.; Lee, T.; Reed, M. A. *Phys. Rev. B: Condens. Matter Mater. Phys.* **2003**, *68*, 035411−035417.

(33) Sachs, S. B.; Dudek, S. P.; Hsung, R. P.; Sita, L. R.; Smalley, J. F.; Newton, M. D.; Feldberg, S. W.; Chidsey, C. E. D. *J. Am. Chem. Soc.* **1997**, *119*, 10563−10564.

(34) Wold, D. J.; Haag, R.; Rampi, M. A.; Frisbie, C. D. *J. Phys. Chem. B* **2002**, *106*, 2813−2816.

(35) Cohen, R.; Stokbro, K.; Martin, J. M. L.; Ratner, M. A. *J. Phys. Chem. C* **2007**, *111*, 14893−14902.

(36) Berchmans, S.; Yegnaraman, V.; Rao, G. P. *J. Solid State Electrochem.* **1998**, *3*, 52−54.

(37) Malkhandi, S.; Yang, B.; Manohar, A. K.; Prakash, G. K.; Narayanan, S. R. *J. Am. Chem. Soc.* **2013**, *135*, 347−353.

(38) Yang, B.; Malkhandi, S.; Manohar, A. K.; Surya Prakash, G. K.; Narayanan, S. R. *Energy Environ. Sci.* **2014**, *7*, 2753−2763.

(39) Dai, Z.; Ju, H. *Phys. Chem. Chem. Phys.* **2001**, *3*, 3769−3773.

(40) Zharnikov, M.; Grunze, M. *J. Phys.: Condens. Matter* **2001**, *13*, 11333−11365.

(41) Conway, B. E. *Proc. R. Soc. London, Ser. A* **1960**, *256*, 128−144.

(42) Ozaki, A. *Isotopic Studies of Heterogeneous Catalysis*; Kodansha Ltd.: Tokyo, 1977; p 183.

(43) Guena, T.; Pletcher, D. *Acta Chem. Scand.* **1998**, *52*, 23−31.

(44) Birkett, M. D.; Kuhn, A. T. The catalytic hydrogenation of organic compounds—a comparison between the gas-phase, liquid-phase, and electrochemical routes. In *Catalysis*; Bond, G. C., Webb, G., Eds.; The Royal Society of Chemistry: London, 1983; Vol. *6*, pp 61−89.

(45) Albert, W. C.; Lowy, A. *Trans. Electrochem. Soc.* **1939**, *75*, 367−375.
(46) Zhou, F.; Bard, A. J. *J. Am. Chem. Soc.* **1994**, *116*, 393−394.
(47) Shi, Y.; Zhu, Y.; Yang, Y.; Li, Y.-W.; Jiao, H. *ACS Catal.* **2015**, *5*, 4020−4032.
(48) Stradins, J. P. *Electrochim. Acta* **1964**, *9*, 711−720.
(49) Horányi, G. *Catal. Today* **1994**, *19*, 285−312.
(50) Pletcher, D.; Razaq, M. *Electrochim. Acta* **1981**, *26*, 819−824.

DOI: 10.1021/jacs.7b06331
J. Am. Chem. Soc. 2017, 139, 14120−14128